J Fluoresc (2012) 22:719–727
DOI 10.1007/s10895-011-1007-z

ORIGINAL PAPER

Development of Novel Nanocarrier-Based Near-Infrared Optical Probes for *In Vivo* Tumor Imaging

Yoichi Shimizu · Takashi Temma · Isao Hara · Ryo Yamahara · Ei-ichi Ozeki · Masahiro Ono · Hideo Saji

Received: 5 September 2011 / Accepted: 18 October 2011 / Published online: 10 November 2011

Abstract Optical imaging with near-infrared (NIR) fluorescent probes is a useful diagnostic technology for *in vivo* tumor detection. Our plan was to develop novel NIR fluorophore-micelle complex probes. IC7-1 and IC7-2 were synthesized as novel lipophilic NIR fluorophores, which were encapsulated in an amphiphilic polydepsipeptide micelle "lactosome". The fluorophore-micelle complexes IC7-1 lactosome and IC7-2 lactosome were evaluated as NIR fluorescent probes for *in vivo* tumor imaging. IC7-1 and IC7-2 were synthesized and then encapsulated in lactosomes. The optical properties of IC7-1, IC7-2, IC7-1 lactosome and IC7-2 lactosome were measured. IC7-1 lactosome and IC7-2 lactosome were administered to tumor-bearing mice, and fluorescence images were acquired for 48 h. IC7-1 and IC7-2 were successfully synthesized in 12% and 6.3% overall yield, and maximum emission wavelengths in chloroform were observed at 858 nm and 897 nm, respectively. Aqueous buffered solutions of IC7-1 lactosome and IC7-2 lactosome showed similar fluorescence spectra in chloroform and higher or comparable quantum yields and higher photostability compared with ICG. Both lactosome probes specifically visualized tumor tissue 6 h post-administration. IC7-1 lactosome and IC7-2 lactosome could be promising NIR probes for *in vivo* tumor imaging.

Y. Shimizu · T. Temma · M. Ono · H. Saji (✉)
Department of Patho-Functional Bioanalysis,
Graduate School of Pharmaceutical Sciences,
Kyoto University,
46-29 Yoshida Shimoadachi-cho, Sakyo-ku,
Kyoto 606-8501, Japan
e-mail: hsaji@pharm.kyoto-u.ac.jp

I. Hara · R. Yamahara · E.-i. Ozeki
Technology Research Laboratory, Shimadzu Corporation,
3-9-4 Soraku-gun, Seika-cho,
Kyoto 619-0237, Japan

Keywords Optical · Near-infrared · Micelle · Molecular imaging

Introduction

Molecular imaging is an evolving field that is progressing from basic research to use in clinical diagnosis [1, 2]. Among several imaging methods, optical imaging can conveniently and safely offer pronounced spatial and temporal resolution that is desirable for *in vivo* applications, especially in the area of cancer imaging. It is notable that near-infrared (NIR) light (700–1,000 nm) transmits deeply through tissues with low scattering, absorption, and auto-fluorescence [3, 4].

Although indocyanine green (ICG, Fig. 1a) is a NIR probe approved by the Food and Drug Administration (FDA) for monitoring cardiac function and hepatic output [5–7], its low quantum yield [4] and low stability in aqueous solution [3] are drawbacks to further applications as an *in vivo* fluorescent molecular probe. ICG derivatives with enhanced lipophilicity could help solve these problems if they were to be utilized in a lipophilic environment, but fluorescent tags for *in vivo* usage should be amenable to an aqueous environment. On the other hand, a polydepsipeptide micelle composed of polysarcosine (PSar) and poly-$_L$-lactic acid (PLLA), named lactosome, has been reported to be an *in vivo* stable, hydrophilic nanocarrier of ~30 nm in diameter, which can encapsulate hydrophobic compounds and effectively deliver them into tumor tissue by an enhanced permeability and retention (EPR) effect with low nonspecific accumulation in the reticuloendothelial system [8, 9]. Thus, our goal was to synthesize lipophilic ICG derivatives possessing better fluorescence properties and encapsulate them in lactosomes to provide NIR probes for *in vivo* tumor imaging.

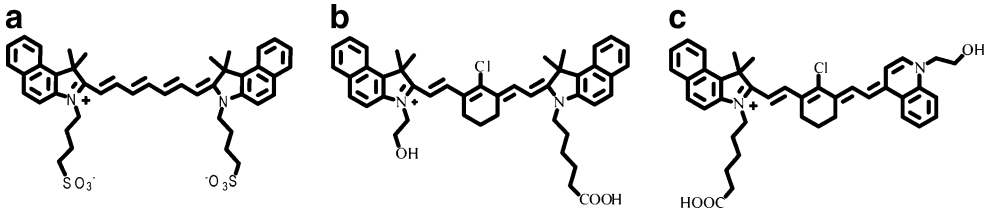

Fig. 1 Chemical structures of ICG (**a**), IC7-1 (**c**) and IC7-2 (**c**)

To develop the novel lipophilic NIR compound, IC7-1 (Fig. 1b), a cyclohexenyl ring was introduced into the polymethine chain of ICG to rigidify the structure and to provide improved photostability and a higher quantum yield [10, 11]. A related asymmetric ICG derivative incorporating a quinoline moiety, IC7-2 (Fig. 1c), which had an elongated emission spectrum, was also synthesized for comparative purposes [12].

Materials and Methods

Materials

Aniline, cyclohexanone, N,N'-dicyclohexylcarbodiimide, sodium hydride, 6-bromohexanoic acid, potassium iodide, sodium acetate, 2-iodoethanol, N-hydroxysuccinimide, N, N-dimethylformamide, and ethanol were purchased from Wako Pure Chemical Industries, Ltd. 1,1,2-Trimethylbenz [e]indole was purchased from Sekisui Medical CO, Ltd. ICG was purchased from Tokyo Chemical Industry Co, Ltd.

Instruments

UV–vis spectra were measured using a UV-1800 (SHIMADZU Corporation, Kyoto, Japan). Mass spectra were acquired on a SHIMADZU LC-MS2010 EV (SHIMADZU Corporation, Kyoto, Japan) and an Axima-CFR plus (SHIMADZU Corporation, Kyoto, Japan). 1H-NMR spectra were recorded on a JEOL ECP-300 (JEOL Ltd., Tokyo, Japan). Fluorescence spectroscopy was performed with a Fluorolog-3 (HORIBA Jobin Yvon Inc., Kyoto, Japan), using a slit width of 5 nm for both excitation and emission measurements.

Synthesis

N-[5-Anilino-3-chloro-2,4-(propane-1,3-diyl)-2, 4-pentadiene-1-ylidene]anilinium Chloride (1)

Phosphorus oxychloride (11 mL, 0.12 mol) was added dropwise to anhydrous DMF (13 mL, 0.17 mol) at 0 °C. After 1 h, cyclohexanone (5.5 mL, 0.053 mol) was added, and the mixture was refluxed for 1 h. After cooling to rt, an aniline/EtOH [1:1 (*v*/*v*), 18 mL] mixture was added dropwise, and the reaction was continued at rt for 30 min. The mixture was poured into ice cold H_2O/HCl (10:1, 110 mL), and the resulting residue was filtered, washed with cold H_2O and THF, and then dried *in vacuo* to obtain compound **1** (10.2 g, 53.6%); ^{1}H NMR (DMSO-d_6, 300 MHz) δ8.54 (s, 2H), 7.6-7.2 (m, 10H), 2.74 (t, 4H), 1.85 (m, 2H).

3-(5-Carboxy-pentyl)-1,1,2-trimethyl-1H-benz[e]indolium iodide (2)

6-Bromohexanoic acid (8.4 g, 43.0 mmol) and potassium iodide (7.2 g, 43 mmol) were dissolved in toluene (5 mL). After addition of 1,1,2-trimethyl-1*H*-benz[*e*]indole (3.0 g, 14.3 mmol), the mixture was refluxed for 15 h. The resulting precipitate was washed with THF, chilled H_2O, and chloroform and then dried *in vacuo* to obtain compound **2** (5.0 g, 77%); ^{1}H NMR (CD_3OD) 8.33 (d, 1H, J=8.5), 8.24 (d, 1H, J=8.8), 8.16 (d, 1H, J=8.3), 8.02 (d, 1H, J=8.8), 7.8 (t, 1H, J=7.2), 7.71 (t, 1H, J=7.2), 4.64 (t, 2H, J=7.7), 2.35 (t, 2H, J=6.9), 2.0-1.9 (m, 2H), 1.84 (s, 6H), 1.75-1.65 (m, 2H), 1.65-1.55 (m, 2H).

2-[4'-Chloro-6'-(N-phenyl)-3',5'-trimethyleneheptatrien-1-yl]-1-(5-Carboxy-pentyl)-1,1,2-trimethyl-1H-benz[e] indolium iodide (3)

A mixture of compound **1** (3.00 g, 8.35 mmol), **2** (3.77 g, 8.35 mmol) and anhydrous sodium acetate (0.753 g, 9.19 mmol) in anhydrous EtOH (75 mL) was refluxed for 6 h under a N_2 atmosphere. After the reaction was complete, the mixture was neutralized with 0.2 M phosphate buffer (pH 7.0), and then extracted with chloroform. The extract was evaporated, and the residue was purified by column chromatography to obtain compound **3** (1.45 g, 25.5%); ^{1}H NMR (CD_3OD) δ8.56 (s, 1H), 8.2-8.1 (m, 2H), 7.95-7.85 (m, 2H), 7.6-7.1 (m, 8H), 6.10 (d, 1H, J=13.8), 4.17 (t, 2H, J=7.2), 2.71 (t, 4H, J=5.8), 2.27 (t, 2H, J=7.4), 2.0-1.8 (m, 4H), 1.93 (s, 6H), 1.8-1.6 (m, 2H), 1.6-1.4 (m, 2H): MS (ESI, pos.) m/z calcd for $C_{35}H_{38}ClN_2O_2$ 554 (M^+), found 554.

3-(2-Hydroxyethyl)-1,1,2-trimethyl-1H-benz[e]indolium iodide (4)

1,1,2-Trimethyl-1*H*-benz[*e*]indole (2.0 g, 9.556 mmol) was dissolved in dry toluene (10 mL) at 80 °C under a N_2 atmosphere. To the solution was added 2-iodoethanol (1.64 g, 9.556 mmol), and the mixture was refluxed for 2 h. After cooling to rt, a slightly blue residue was collected, washed with toluene, and then dried *in vacuo* to obtain compound **4** (1.21 g, 33%); ^{1}H NMR (DMSO-d_6) δ8.39 (d, 1H, J=8.0), 8.29 (d, 1H, J=8.8), 8.22 (d, 1H, J=8.0), 8.14 (d, 1H, J=9.1), 7.79 (t, 1H, J=7.2), 7.73 (t, 1H, J=6.9), 4.72 (t, 2H, J=4.7), 3.94 (t, 2H, J=4.7), 2.93 (s, 3H), 1.78 (s, 6H).

1-(2-Hydroxyethyl)-4-methylquinolinium iodide (5)

A mixture of 4-methylquinoline (1 g, 7 mmol) and 2-iodoethanol (1.2 g, 7 mmol) in dry toluene (5 mL) was stirred at 80 °C under a N_2 atmosphere for 4 h. After cooling, a yellow residue was collected, washed with toluene, and then dried *in vacuo* to obtain compound **5** (1.63 g, 74%); ^{1}H NMR (CD_3OD) δ9.14 (d, 1H, J=6.3), 8.62-8.52 (m, 2H), 8.25 (t, 1H, J=6.3), 8.06 (t, 1H, J=6.2), 7.97 (d, 1H, J=6.0), 5.14 (t, 2H, J=4.9), 4.08 (t, 2H, J=5.0), 3.07 (s, 3H).

2-[4'-Chloro-7'-(1"-(2-Hydroxyethyl)-1,1,2-trimethyl-1H-benz[e]indolium)-3',5'-trimethyleneheptatrien-1-yl]-1-(5-Carboxypentyl)-1,1,2-trimethyl-1H-benz[e]indolium iodide (IC7-1)

A mixture of compound **3** (1.16 g, 1.70 mmol), **4** (0.714 g, 1.87 mmol), and anhydrous sodium acetate (0.153 g, 1.87 mmol) in anhydrous EtOH (29 mL) was refluxed for 5 h under a N_2 atmosphere. After the reaction was complete, the mixture was neutralized with 0.2 M phosphate buffer (pH 7.0) and then extracted with chloroform. The organic extract was evaporated, and the residue was purified by column chromatography to obtain IC7-1 (1.22 g, 85.3%); ^{1}H NMR (CD_3OD) δ8.54 (m, 2H), 8.26 (t, 2H, J=8.1), 8.05-7.95 (m, 4H), 7.7-7.4 (m, 6H), 6.46 (d, 1H, J=14.3), 6.28 (d, 1H, J=14.0), 4.42 (t, 2H, J=5.0), 4.28 (t, 2H, J=8.0), 4.03 (t, 2H, J=5.0), 2.75 (t, 4H, J=5.8), 2.31 (t, 2H, J=7.2), 2.1-1.8 (m, 6H), 2.05 (s, 6H), 2.01 (s, 6H), 1.8-1.6 (m, 2H), 1.6-1.4 (m, 2H): MS (ESI, pos) m/z calcd for $C_{46}H_{50}ClN_2O_3$ 714 (M^+), found 714.

IC7-1-NHS

To a solution of IC7-1 (600 mg, 0.713 mmol) in anhydrous DMF (12 mL) was added dicyclohexylcarbodiimide (DCC, 440 mg, 2.14 mmol) at 0 °C. The reaction was stirred for 20 min, and then N-hydroxysuccinimide (NHS, 246 mg, 2.14 mmol) was added. The solution was gradually allowed to warm to room temperature, and it was stirred for 2 days. After the reaction was complete, ethyl acetate was added to the mixture, and the dicyclohexylurea was removed by filtration. The solution was evaporated, and the residue was purified by flash chromatography to obtain IC7-1-NHS (100 mg, 14.9%); ^{1}H NMR (CD_3OD) δ8.50 (m, 2H), 8.23 (t, 2H, J=8.1), 8.1-7.9 (m, 4H), 7.7-7.4 (m, 6H), 6.45 (d, 1H, J=14.3), 6.24 (d, 1H, J=14.3), 4.41 (t, 2H, J=5.0), 4.24 (t, 2H, J=8.0), 4.03 (t, 2H, J=4.9), 2.8-2.6 (m, 6H), 2.78 (s, 4H), 2.0-1.5 (m, 8H), 2.01 (s, 6H), 1.99 (s, 6H): MS calcd for $C_{50}H_{53}ClN_3O_5$ (M^+) 811, found 811.

2-[4'-Chloro-7'-(1"-(2-Hydroxyethyl)-4-methylquinolinium)-3',5'-trimethyleneheptatrien-1-yl]-1-(5-Carboxypentyl)-1,1,2-trimethyl-1H-benz[e]indolium iodide (IC7-2)

A mixture of compound **3** (414 mg, 0.608 mmol), **5** (210.7 mg, 0.669 mmol), and anhydrous sodium acetate (54.9 mg, 0.669 mmol) in anhydrous EtOH (12 mL) was refluxed for 8 h under a N_2 atmosphere. After the reaction was complete, the mixture was neutralized with 0.2 M phosphate buffer (pH 7.0) and then extracted with chloroform and methanol. The organic extract was evaporated, and the residue was purified by column chromatography to obtain IC7-2 (221 mg, 46.7%); ^{1}H NMR (CD_3OD) δ8.65 (d, 1H, J=6.6), 8.57 (d, 1H, J=8.8), 8.39 (d, 1H, J=15.1), 8.26 (d, 1H, J=8.8), 8.15-7.65 (m, 7H), 7.44 (t, 1H, J=7.4), 7.35-7.1 (m, 3H), 5.69 (d, 1H, J=13.4), 4.05 (t, 2H, J=4.7), 3.83 (t, 2H, J=6.9), 2.8-2.65 (m, 4H), 2.21 (t, 2H, J=7.4), 1.90 (s, 6H), 2.0-1.6 (m, 7H), 1.6-1.2 (m, 3H): MS (ESI, pos) m/z calcd for $C_{41}H_{44}ClN_2O_3$ (M^+) 647, found 647.

IC7-2-NHS

To a solution of IC7-2 (355 mg, 0.457 mmol) and NHS (157.7 mg, 1.370 mmol) in anhydrous DMF (3.5 mL) was added DCC (188.5 mg, 0.914 mmol), and the mixture was stirred for 1 h at 0 °C. The solution was allowed to gradually warm to room temperature, and it was stirred for 2.5 days. After the reaction was complete, ethyl acetate was added to the mixture, and the dicyclohexylurea was removed by filtration. The filtrate was evaporated, and the residue was purified by flash chromatography to obtain IC7-2-NHS (62 mg, 15.6%); ^{1}H NMR (CD_3OD) δ8.64 (d, 1H, J=6.6), 8.56 (d, 1H, J=8.5), 8.34 (d, 1H, J=12.4), 8.25 (d, 1H, J=8.8), 8.15-7.65 (m, 7H), 7.44(t, 1H, J=7.4), 7.35-7.1 (m, 3H), 5.69 (br, 1H), 4.04 (t, 2H, J=4.7), 3.83 (br, 2H), 2.66 (s, 4H), 2.9-2.50 (m, 6H), 1.90 (s, 6H), 2.0-1.6 (m, 7H), 1.6-1.2 (m, 3H): MS (ESI, pos) m/z calcd for $C_{45}H_{47}ClN_3O_5$ (M^+) 744, found 744.

Preparation of IC7-1 or IC7-2 encapsulated lactosomes

To a solution of IC7-1-NHS (1.1 mg, 1.68 μmol) or IC7-2-NHS (1.0 mg, 1.68 μmol) in anhydrous DMF (1 mL) was added $PLLA_{30}$ bearing a free amino group (3.45 mg, 1.52 μmol). The solution was stirred at room temperature overnight while shielding the reaction from light, and the resulting mixture was purified by size exclusion chromatography (Sephadex LH-20 column) using DMF as eluant. The fraction of high molecular mass was collected and dried *in vacuo*. IC7-1-PLLA: MS (MALDI-TOF, pos) m/z calcd for $C_{50}H_{53}ClN_3O_5$ ($[M+H]^+$) 2958, found 2958. IC7-2-PLLA: MS (MALDI-TOF, pos) m/z calcd for $C_{135}H_{172}ClN_4O_{63}$ (M^+) 2895, found 2895.

The amphiphilic polymer $PLLA_{30}$-block-$PSar_{70}$ (Fig. 2) was supplied by the Shimadzu Corporation. A chloroform (1 mL) solution of the polymer (388 nmol) and IC7-1-PLLA (3.9 nmol) or IC7-2-PLLA (3.9 nmol) was dripped into a glass test tube. The solvent was removed under reduced pressure to form a thin film on the walls of the tube. PBS buffer (0.1 M, pH 7.4) was added to the test tube, and the tube was heated at 82 °C for 20 min. The resulting aqueous solution was filtered through a 0.20 μm Acrodisc® syringe filter (Pall Corp, East Hills, NY). The size distribution of IC7-1 lactosome and IC7-2 lactosome was measured at 25 °C using a Zetasizer Nano-S90 (Malvern instruments Ltd., UK). The purities of IC7-1 lactosome and IC7-2 lactosome were measured by size exclusion chromatography using a Superdex 200 10/300 GL column (GE Healthcare, U.K.) equilibrated with PBS (−) at a flow rate of 0.5 ml/min. Absorbances at 215 nm and 830 nm were used for detection of the lactosome and IC7-1/IC7-2, respectively.

Optical characteristics of IC7-1, IC7-1 lactosome, IC7-2 and IC7-2 lactosome

The log P values of IC7-1, IC7-2, and ICG were calculated by ACD/Labs ver. 11.0 (Advanced Chemistry Development, Inc., Toronto, Canada).

The fluorescence emission spectra of IC7-1 and IC7-2 (10 μM) were measured in methanol and chloroform at 25 °C, following excitation at 815 nm and 820 nm, respectively. Fluorescence emission spectra of IC7-1 lactosome and IC7-2 lactosome (1.3 μM) were measured in H_2O at 25 °C, following excitation at 815 nm and 820 nm, respectively. Quantum yields for IC7-1, IC7-1 lactosome, IC7-2, and IC7-2 lactosome were acquired by a sphere accessory equipped with a Fluorolog-3 (HORIBA Jobin Yvon Inc., Kyoto, Japan). Excitation spectra of IC7-1 and IC7-2 (10 μM) were measured in methanol and chloroform at 25 °C following emission at 880 nm and 900 nm, respectively, and those of IC7-1 lactosome and IC7-2 lactosome (1.3 μM) were measured in H_2O at 25 °C following excitation at 880 nm and 890 nm, respectively. Absorption spectra of IC7-1 and IC7-2 (10 μM) were measured in methanol and chloroform at 25 °C, and those of IC7-1 lactosome and IC7-2 lactosome were measured in water at 25 °C.

The photostability of IC7-1 lactosome, IC7-2 lactosome, and ICG were evaluated by a decrease of absorbance over time. IC7-1 lactosome (1.3 μM in H_2O), IC7-2 lactosome (1.3 μM in H_2O) and ICG (1.3 μM in H_2O) were continuously illuminated with a tungsten lamp in a visible-ultraviolet spectrophotometer (UV-1800) for 1 h. The absorption was measured at the corresponding wavelengths (IC7-1 lactosome: 830 nm, IC7-2 lactosome: 830 nm, and ICG: 780 nm) every 0.1 min for 1 h after UV illumination was initiated.

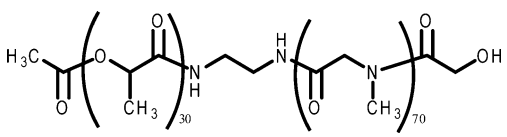

Fig. 2 Chemical structure of the amphiphilic block polymer ($PLLA_{30}$-block-$PSar_{70}$)

Tumor bearing mice

Female nude mice (BALB/c nu/nu) supplied by Japan SLC, Inc. (Hamamatsu, Japan), were housed under a 12-h light/12-h dark cycle and were given free access to food and water. Animal experiments in this study were conducted in accordance with institutional guidelines and were approved by the Kyoto University Animal Care Committee, Japan. FM3A cells were supplied by the Health Science Research Resources Bank (HSRRB) (Osaka, Japan). The cell lines were cultured in DMEM medium with 10% fetal bovine serum at 37 °C in a humidified atmosphere containing 5% CO_2. FM3A cells, 5×10^6 cells in 100 μL of phosphate-buffered saline (PBS), were subcutaneously inoculated into the right hind legs of 7-week-old nude mice. Tumor bearing mice 12 days after transplantation were used for the imaging study.

In vivo imaging study

IC7-1 lactosome and IC7-2 lactosome (1.7 μM, 200 μL) were injected into groups of three tumor-bearing mice, and NIRF images were obtained using a Clairvivo OPT (SHIMADZU Corporation, Kyoto, Japan) with a 785 nm single laser (IC7-1 lactosome) or 808 nm single laser (IC7-2 lactosome) for excitation and a 845/55 nm band-path filter (IC7-1 lactosome) or 850 nm long-path filter (IC7-2 lactosome) for emission. During the imaging process, mice

were kept on the imaging stage under anesthesia using a 2.5% isoflurane gas in oxygen flow (1.5 L/min). For image analysis, Clairvivo OPT measurement and display software ver. 2.00 (SHIMADZU Corporation, Kyoto, Japan) was used. Regions of interest (ROI) were designated for the tumor and muscle (the left hind leg) on the back images and for the liver on the front images. The average signal intensity values were recorded for each ROI and were plotted versus time.

Statistics

Data are presented as means±S.D. Statistical analysis of the photostability of IC7-1 lactosome and IC7-2 lactosome vs ICG was performed with two-way factorial ANOVA followed by the Tukey-Kramer test. Statistical analyses for fluorescence intensities of tumor vs muscle or liver of mice administered IC7-1 lactosome or IC7-2 lactosome were performed with two-way factorial ANOVA followed by the Tukey-Kramer test.

Results

Synthesis of IC7-1, IC7-2, IC7-1 lactosome and IC7-2 lactosome

IC7-1 and IC7-2 were synthesized from cyclohexanone and 1,1,2-trimethyl-1*H*-benz[*e*]indole, as shown in Scheme 1, in 12% and 6.3% overall yield. The calculated log P values of IC7-1 and IC7-2 were 3.62 and 0.90, respectively, while the clog P of ICG was −1.69. To allow these fluorophores to dissolve in aqueous solvent, they were encapsulated in lactosomes using a film rehydration technique. The preparation of IC7-1 lactosome and IC7-2 lactosome was confirmed by size exclusion chromatography using Superdex 200 10/300 GL (GE Healthcare, U.K.), and dual absorbance peaks at 280 nm (lactosome) and 830 nm (IC7-1/IC7-2) were only seen in the higher molecular weight fraction (4–5 min). The particle sizes of IC7-1 lactosome and IC7-2 lactosome were 33.4±3.1 nm (n=6) and 39.6±1.9 nm (n=4), respectively.

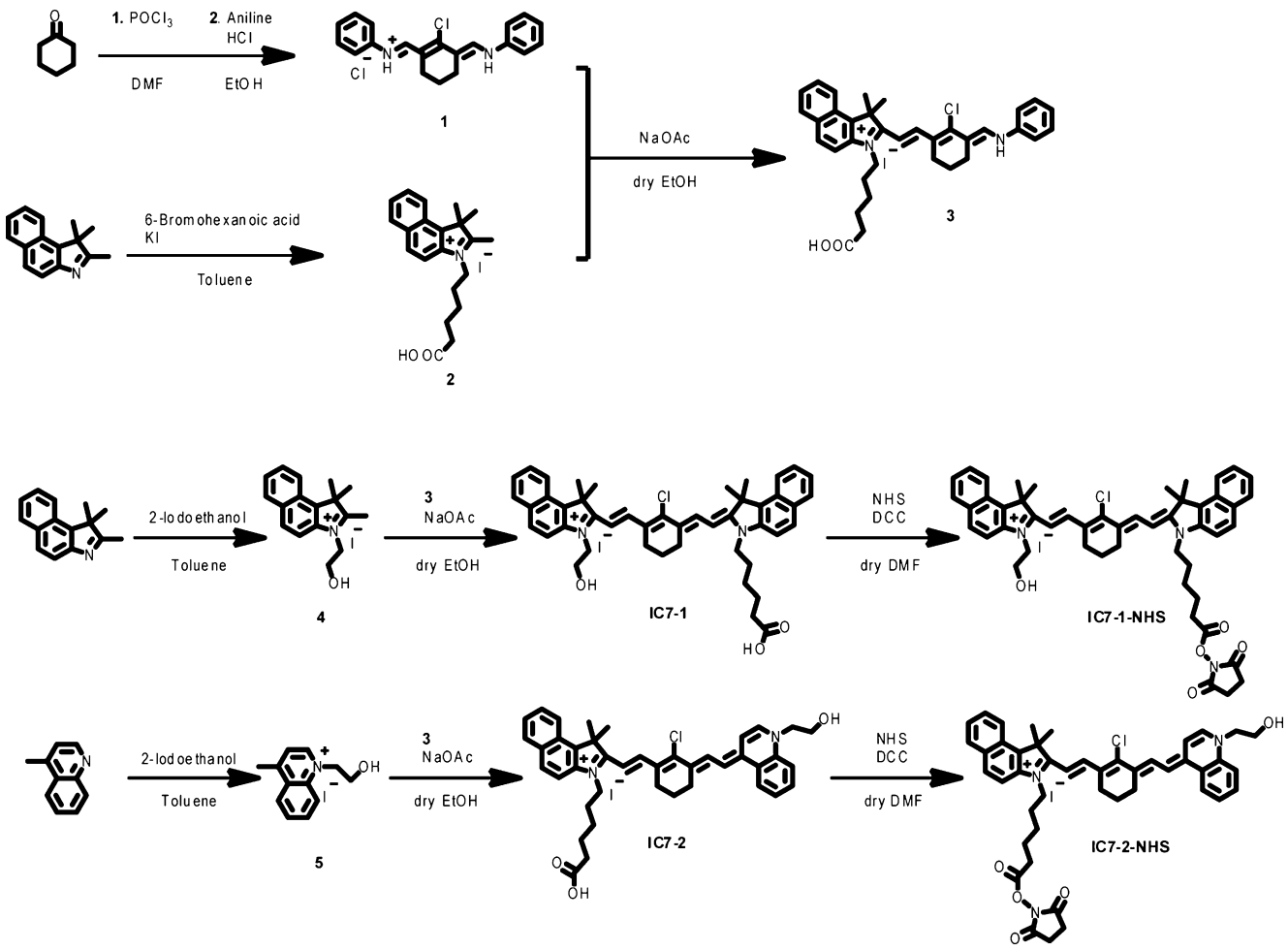

Scheme 1 Synthetic scheme for the preparation of IC7-1, IC7-2 and NHS derivatives

Fluorescence characteristics of IC7-1, IC7-2, IC7-1 lactosome and IC7-2 lactosome

IC7-1, a lipophilic fluorophore with a cyclohexene ring in the interior of the polymethine chain of the ICG structure, had a maximum emission wavelength at 858 nm in chloroform (Table 1). IC7-2 with an unsymmetrical cyanine structure had a maximum emission wavelength at 897 nm in chloroform, which as expected was a longer emission wavelength compared with conventional NIR-dyes. In addition to maximum emission wavelength, other fluorescent properties of IC7-1 and IC7-2 in chloroform such as fluorescence spectrum, quantum yield, and extinction coefficient were also quite similar to those of IC7-1 lactosome and IC7-2 lactosome measured in water (Fig. 3, Table 1). In particular, IC7-1 and IC7-1 lactosome had sharp absorbance and emission spectra and a narrow Stokes shift, while IC7-2 and IC7-2 lactosome had broad absorption spectra and a relatively long Stokes shift.

The fluorescence characteristics of IC7-1, IC7-1 lactosome, IC7-2, and IC7-2 lactosome were compared with ICG as summarized in Table 1. Both IC7-1 and IC7-2 displayed longer absorbance, excitation, and emission wavelengths than ICG. IC7-1 and IC7-2 had higher quantum yields and molar extinction coefficients in chloroform than in methanol. IC7-1 lactosome had approximately 52 nm and 43 nm longer maximum absorbance and emission wavelengths and approximately 2.5 fold higher quantum yield and molar extinction coefficients compared with ICG. IC7-2 lactosome had a maximum emission wavelength that was 55 nm longer than IC7-1 lactosome and 98 nm longer than ICG.

Regarding photostability of the three probes, the absorbances of IC7-1 lactosome and IC7-2 lactosome were stable for 1 h under tungsten lamp irradiation (Fig. 4). On the other hand, the absorbance of ICG significantly decreased in a time-dependent manner ($p<0.0001$), and the normalized absorbance of ICG after 60 min was 61% of the 0 min value.

In vivo imaging study

Fluorescence images of tumor-bearing mice administered IC7-1 lactosome or IC7-2 lactosome are shown in Fig. 5a and b, respectively. The tumors of mice administered IC7-1 lactosome and IC7-2 lactosome were visible with both agents 6 h after administration. The fluorescence intensity at the tumor region of mice administered IC7-1 lactosome (Fig. 5c) and IC7-2 lactosome (Fig. 5d) gradually increased in a time-dependent manner reaching a peak 24 h after administration that was significantly greater than the fluorescence observed in the muscle and liver regions ($p< 0.05$). The fluorescence intensities of tumors 24 h after probe administration were 3.1 fold (IC7-1 lactosome) and 2.5 fold (IC7-2 lactosome) greater than those at the 0 h time point (immediately after probe administration). The intensities in the muscle region (the opposite side from the tumor) were relatively constant during the study, and the tumor-to-muscle fluorescence ratios 24 h after administration were 2.2±0.7 (IC7-1 lactosome) and 2.2±0.2 (IC7-2 lactosome). The tumor-to-liver fluorescence ratios 24 h after administration were 2.5±0.6 (IC7-1 lactosome) and 1.7±0.2 (IC7-2 lactosome), while the intensities in the liver region of the IC7-2 lactosome group were transiently high during the early imaging phase.

Discussion

In this study, two lipophilic NIR fluorescent agents, IC7-1 and IC7-2, were prepared and evaluated (Fig. 1). To enhance the utility of these agents for *in vivo* NIR optical tumor imaging, they were encapsulated in a lactosome formulation to take advantage of the ability of lactosomes to effectively target and deliver lipophilic compounds to tumor tissues. As expected, these fluorescent probes and their lactosome complexes displayed absorption, excitation, and emission spectra with red shifts (Fig. 3) as well as high photostability compared with ICG (Fig. 4). The IC7-1

Table 1 Optical properties of IC7-1, IC7-1 lactosome, IC7-2, IC7-2 lactosome, and ICG

Entry	Solvent	Abs_{max}	Ex_{max}	Em_{max}	Quantum yield	Extinction coefficient (M^{-1} cm^{-1})
IC7-1	$CHCl_3$	829	830	858	0.054	2.1×10^5
	MeOH	819	823	840	0.021	1.2×10^5
IC7-1 lactosome	H_2O	831	831	850	0.059	2.2×10^5
IC7-2	$CHCl_3$	781	805	897	0.008	9.2×10^4
	MeOH	790	883	932	0.001	2.6×10^4
IC7-2 lactosome	H_2O	830	844	905	0.014	6.0×10^4
ICG	H_2O	779	762	807	0.023	7.8×10^4

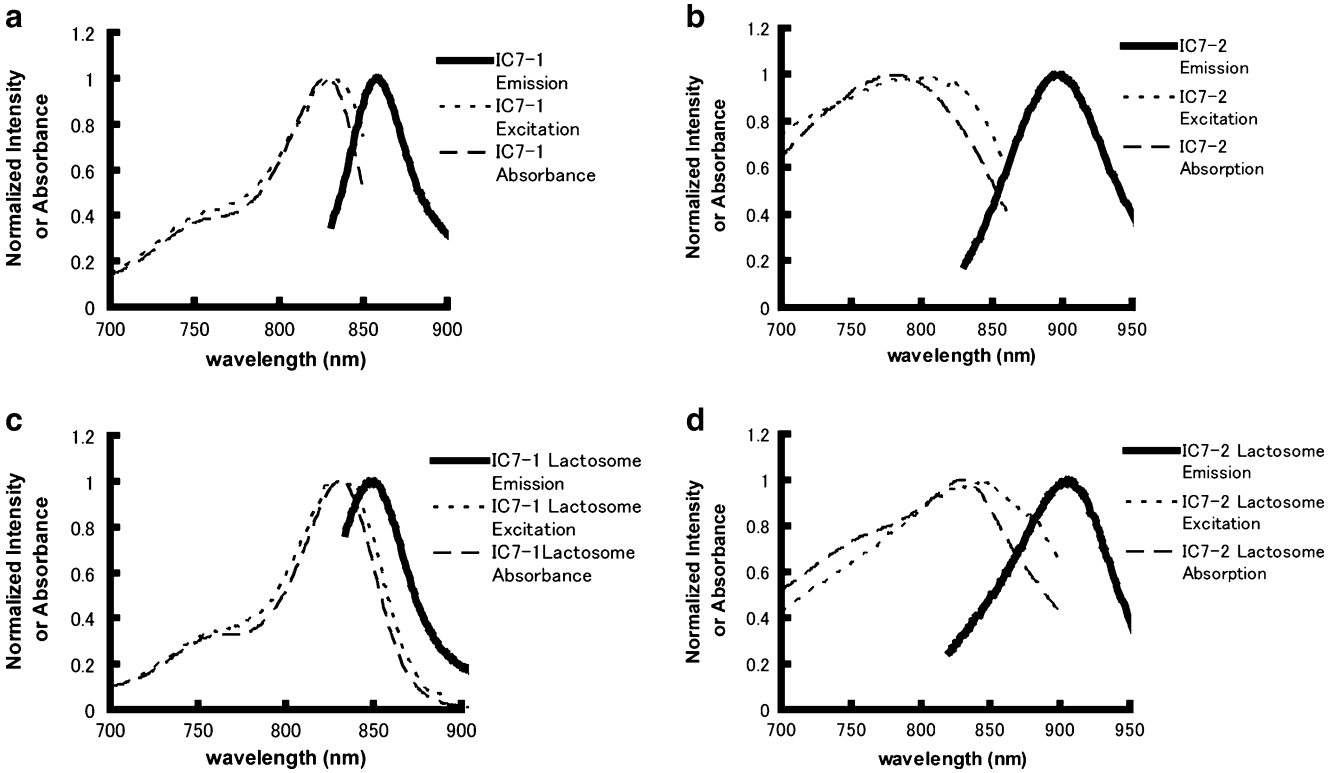

Fig. 3 Emission (*solid line*), excitation (*dotted line*) and absorption (*dotted solid line*) spectra of IC7-1 (**a**), IC7-2 (**b**), IC7-1 lactosome (**c**), and IC7-2 lactosome (**d**). The spectra for IC7-1 and IC7-2 were measured in chloroform and the spectra for IC7-1 lactosome and IC7-2 lactosome were measured in water

lactosome possessed a 2.5 fold higher quantum yield than ICG in aqueous solution (Table 1). In addition, IC7-1 lactosome and IC7-2 lactosome clearly allowed visualization of tumor tissue 6 h post-administration and showed significant fluorescence intensity in tumor tissue 24 h and 48 h after administration (Fig. 5).

In the design of IC7-1, a cyclohexene ring was incorporated into the interior of the polymethine chain of the ICG structure, because the added structural rigidity provided by a ring would lead to a red-shift of the emission and would increase the photostability and quantum yield in a lipophilic environment [13]. As a result of this modification, the emission spectra were elongated approximately 50 nm compared with ICG. IC7-2 was designed with similar functional groups as IC7-1, but with an unsymmetrical structure, by replacing one of the hetero-tricyclic moieties of IC7-1 with a quinoline ring, since it has previously been reported that unsymmetrical fluorogenic cyanines typically have longer wavelength emission spectra [12, 14] than the corresponding symmetrical cyanines. As expected, a longer emission wavelength (ca 900 nm) was observed for IC7-2 compared to IC7-1, which could provide superior properties for *in vivo* usage, although the quantum yield of IC7-2 was somewhat lower than IC7-1.

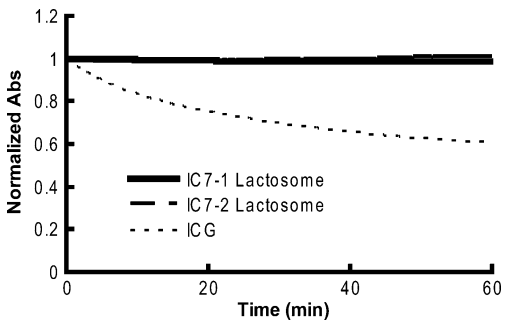

Fig. 4 Photostability of IC7-1 lactosome (*bold line*), IC7-2 lactosome (*dotted bold line*), and ICG (*dotted line*)

Multicolor *in vivo* optical imaging is a promising technique for detecting different tumor types or lymph nodes simultaneously [15, 16]. Since NIR fluorescent organic compounds that are commercially available or that have been reported for *in vivo* optical imaging have emission wavelengths in the range of 650–820 nm [17], and widely used quantum dot based agents have toxicity concerns due to associated heavy metals [18, 19], our probes with emission spectra in the 800–900 nm range offer a possible alternative for multicolor *in vivo* optical imaging.

To make IC7-1 and IC7-2 more effective for use in an aqueous environment while maintaining their optical properties, the fluorophores were encapsulated in nano-

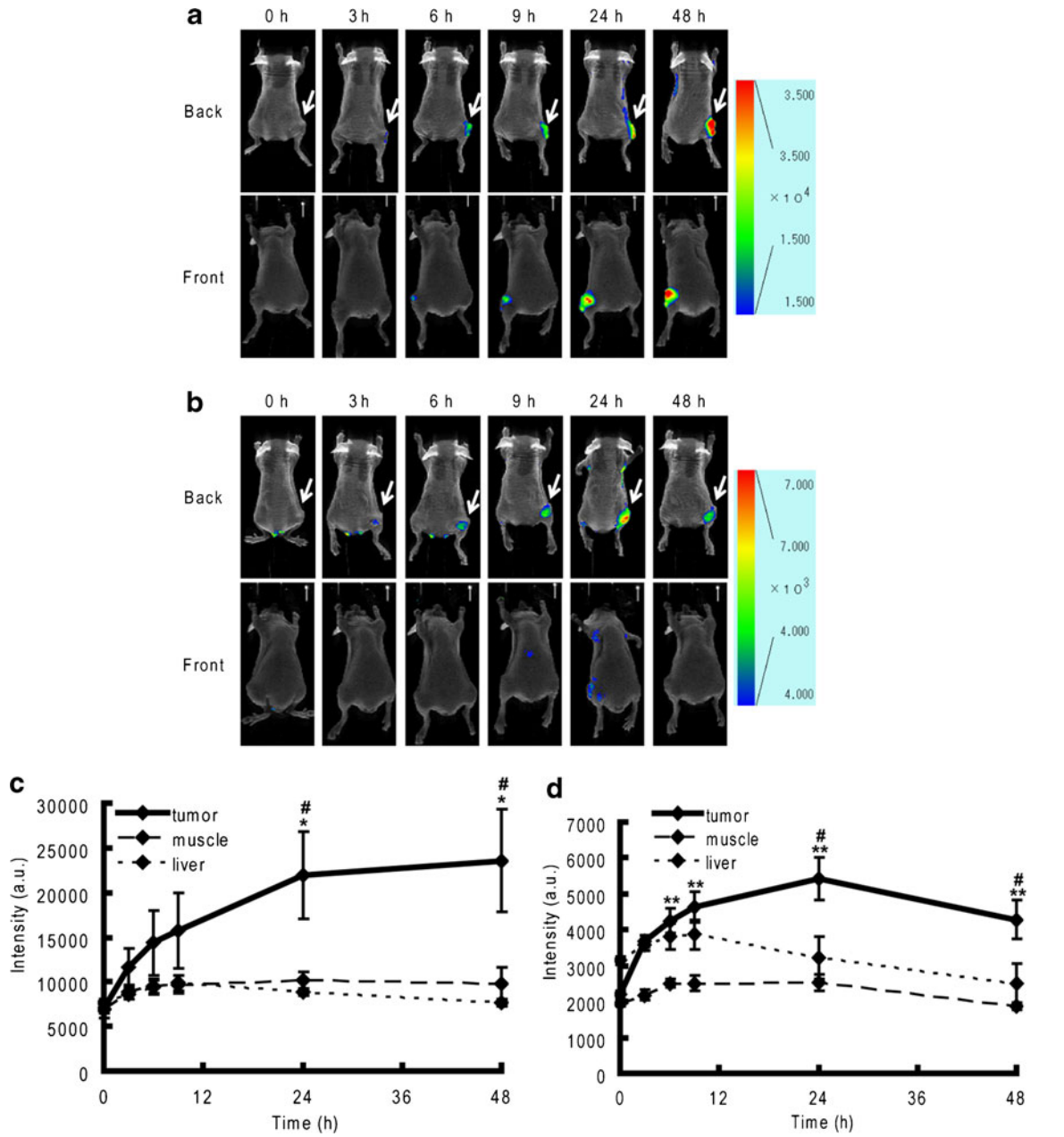

Fig. 5 **a, b** Back (*upper*) and front (*lower*) fluorescence images of FM3A cell xenografted mice at 0 h (just after injection), 3, 6, 9, 24, and 48 h after administration of IC7-1 lactosome (**a**) and IC7-2 lactosome (**b**). The *arrows* indicate the tumor (**c**, **d**). Fluorescence intensities at the region of interest of the tumor, muscle, and liver of mice administered IC7-1 lactosome (**c**) and IC7-2 lactosome (**d**). Data are expressed as fluorescence intensity (mean±S.D.). Comparisons of the fluorescence intensities of tumor and muscle or liver were performed with two-way factorial ANOVA followed by the Tukey-Kramer test (*$p<0.05$ vs. muscle, **$p<0.01$ vs muscle, $^{\#}p<0.05$ vs. liver)

carriers. As a nanocarrier for the imaging agents, we chose an amphiphilic polydepsipeptide micelle "lactosome". Lactosome has a diameter of approximately 30–40 nm, which is a suitable size for delivery to tumor tissue through the EPR effect [20]. Furthermore, lactosomes have the ability to escape the reticuloendothelial system (RES), and thus, they are able to suppress nonspecific accumulation of the probes in the abdominal region [21]. Experimental results showed that IC7-1 lactosome and IC7-2 lactosome had better quantum yields and photostability and longer (more favorable for *in vivo* imaging usage) excitation/emission wavelengths than ICG under aqueous conditions, which suggested that the high lipophilicity of IC7-1 and IC7-2 was adequate for encapsulation in lactosomes, i.e. the hydrophobic core of the lactosome provided a suitable environment for IC7-1 and IC7-2 to exert their favorable optical properties. As clearly demonstrated in the *in vivo* study, selective and pronounced signaling by the newly

developed NIR lactosome probes in tumors and low background signals in liver and muscle tissue were observed and semi-quantified. In addition, lactosome has low toxicity since it is composed of biodegradable substances, poly-sarcosine and poly-$_L$-lactic acid [22, 23]. Therefore, IC7-1 lactosome and IC7-2 lactosome appear to be promising, widely applicable nanocarrier probes for noninvasive *in vivo* imaging techniques.

In this study, highly sensitive *in vivo* tumor imaging with IC7-1 lactosome and IC7-2 lactosome by virtue of the EPR effect was achieved. Regions of inflammation are known to accumulate macromolecules since vascular permeability is facilitated compared with normal tissues [24]; thus, these probes certainly visualized such areas (data not shown). Although tumor accumulation of a probe due to the EPR effect is useful for detecting the presence of tumors and for treatment by drugs carried within the probe, functional imaging that targets functional molecules specifically expressed at the lesion site could further enhance the specific diagnosis of disease, a current trend toward personalization of patient treatment. Thus, studies concerning the conjugation of targeting moieties to the lactosome probes developed in this study are now in progress.

Conclusion

In this study, we synthesized IC7-1 lactosome and IC7-2 lactosome, which had suitable optical imaging properties and achieved clear *in vivo* tumor imaging in mice. Results from the application of IC7-1 lactosome and IC7-2 lactosome as *in vivo* imaging agents indicate that these probes could be beneficial for the clinical detection of tumors.

Acknowledgement This study was supported by Grants-in-Aid for Scientific Research from the Ministry of Education, Culture, Sports, Science, and Technology, Japan. Part of this study was supported by the New Energy and Industrial Technology Development Organization (NEDO), Japan. We thank Dojindo Laboratories (Kumamoto, Japan) for supporting the syntheses of IC7-1 and IC7-2.

References

1. Weissleder R, Pittet MJ (2008) Imaging in the era of molecular oncology. Nature 452(7187):580–589
2. Willmann JK, van Bruggen N, Dinkelborg LM, Gambhir SS (2008) Molecular imaging in drug development. Nat Rev Drug Discov 7(7):591–607
3. Ntziachristos V, Ripoll J, Wang LV, Weissleder R (2005) Looking and listening to light: the evolution of whole-body photonic imaging. Nat Biotechnol 23(3):313–320
4. Weissleder R (2001) A clearer vision for *in vivo* imaging. Nat Biotechnol 19(4):316–317
5. Dzurinko VL, Gurwood AS, Price JR (2004) Intravenous and indocyanine green angiography. Optometry 75(12):743–755
6. Landsman ML, Kwant G, Mook GA, Zijlstra WG (1976) Light-absorbing properties, stability, and spectral stabilization of indocyanine green. J Appl Physiol 40(4):575–583
7. Sakka SG (2007) Assessing liver function. Curr Opin Crit Care 13 (2):207–214
8. Makino A, Kizaka-Kondoh S, Yamahara R, Hara I, Kanzaki T, Ozeki E, Hiraoka M, Kimura S (2009) Near-infrared fluorescence tumor imaging using nanocarrier composed of poly(L-lactic acid)-block-poly(sarcosine) amphiphilic polydepsipeptide. Biomaterials 30(28):5156–5160
9. Makino A, Yamahara R, Ozeki E, Kimura S (2007) Preparation of novel polymer assemblies, "lactosome", composed of Poly(L-lactic acid) and poly(sarcosine). Chem Lett 36(10):1220–1221
10. Lee H, Mason JC, Achilefu S (2006) Heptamethine cyanine dyes with a robust C–C bond at the central position of the chromophore. J Org Chem 71(20):7862–7865
11. Strekowski L, Lipowska M, Patonay G (1992) Substitution reactions of a nucleofugal group in heptamethine cyanine dyes. Synthesis of an isothiocyanato derivative for labeling of proteins with a near-infrared chromophore. J Org Chem 57(17):4578–4580
12. Constantin TP, Silva GL, Robertson KL, Hamilton TP, Fague K, Waggoner AS, Armitage BA (2008) Synthesis of new fluorogenic cyanine dyes and incorporation into RNA fluoromodules. Org Lett 10(8):1561–1564
13. Ballou B, Ernst LA, Waggoner AS (2005) Fluorescence imaging of tumors *in vivo*. Curr Med Chem 12(7):795–805
14. Mujumdar RB, Ernst LA, Mujumdar SR, Lewis CJ, Waggoner AS (1993) Cyanine dye labeling reagents: sulfoindocyanine succinimidyl esters. Bioconjug Chem 4(2):105–111
15. Kobayashi H, Koyama Y, Barrett T, Hama Y, Regino CA, Shin IS, Jang BS, Le N, Paik CH, Choyke PL, Urano Y (2007) Multimodal nanoprobes for radionuclide and five-color near-infrared optical lymphatic imaging. ACS Nano 1(4):258–264
16. Koyama Y, Barrett T, Hama Y, Ravizzini G, Choyke PL, Kobayashi H (2007) *In vivo* molecular imaging to diagnose and subtype tumors through receptor-targeted optically labeled monoclonal antibodies. Neoplasia 9(12):1021–1029
17. Licha K (2002) Contrast agents for optical imaging. Top Curr Chem 222:1–29
18. Derfus AM, Chan CWC, Bhatia SN (2004) Probing the cytotoxicity of semiconductor quantum dots. Nano Lett 4(1):11–18
19. Kirchner C, Liedl T, Kudera S, Pellegrino T, Munoz Javier A, Gaub HE, Stolzle S, Fertig N, Parak WJ (2005) Cytotoxicity of colloidal CdSe and CdSe/ZnS nanoparticles. Nano Lett 5(2):331–338
20. Matsumura Y, Maeda H (1986) A new concept for macromolecular therapeutics in cancer chemotherapy: mechanism of tumoritropic accumulation of proteins and the antitumor agent smancs. Cancer Res 46(12 Pt 1):6387–6392
21. Senior JH (1987) Fate and behavior of liposomes *in vivo*: a review of controlling factors. Crit Rev Ther Drug Carrier Systems 3 (2):123–193
22. Gupta B, Revagadea N, Hilbornb J (2007) Poly(lactic acid) fiber: an overview. Prog Polym Sci 32(4):455–482
23. Tsai G, Lane HY, Yang P, Chong MY, Lange N (2004) Glycine transporter I inhibitor, N-methylglycine (sarcosine), added to antipsychotics for the treatment of schizophrenia. Biol Psychiatry 55(5):452–456
24. Maeda H, Wu J, Sawa T, Matsumura Y, Hori K (2000) Tumor vascular permeability and the EPR effect in macromolecular therapeutics: a review. J Control Release 65(1–2):271–284